Human Cell (2022) 35:803–816
https://doi.org/10.1007/s13577-022-00678-5

RESEARCH ARTICLE

A20 alleviated caspase-1-mediated pyroptosis and inflammation stimulated by *Porphyromonas gingivalis* lipopolysaccharide and nicotine through autophagy enhancement

Hui Tang[1,2] · Yu Ye[1,2] · Lu Li[1,2] · Yi Zhou[1,2] · Liguang Hou[1,2] · Shuangshuang Ren[1,2] · Yan Xu[1,2]

Received: 4 August 2021 / Accepted: 19 January 2022 / Published online: 25 February 2022

Abstract

Periodontitis is the leading cause of tooth loss, and patients with smoking habits are at an increased risk of developing periodontitis. A20 (the tumor necrosis factor alpha-induced protein 3, TNFAIP3) is one of the key regulators of inflammation and cell death in numerous tissues. Emerging researches indicated A20 as a fundamental molecule in the periodontal tissue. This study was to evaluate the role of A20 against cell death and inflammation in periodontitis and to elucidate the underlying mechanisms. In our study, western blot, autophagy detection, and transmission electron microscopy showed that lipopolysaccharide from *Porphyromonas gingivalis* (*Pg*.LPS) and nicotine (NI) could enhance the activation of autophagy. *Pg*.LPS and NI induce the pyroptosis of human periodontal ligament cells (hPDLCs), as evidenced by the decrease of membrane integrity and the increase of NLRP3, GSDMD, GSDMD-N, caspase-1 activity, and the pro-inflammatory cytokines of IL-1β, IL-6, TNF-α. Further researches were focused on that A20, an ubiquitin-editing enzyme, was linked to hPDLCs pyroptosis. Overexpression or silencing A20 could diminish or aggravate pyroptosis in hPDLCs by the modulation of autophagy. The above results demonstrated that A20 dictated the cross-talk between pyroptosis and autophagy. Overexpression of A20 enhanced autophagy to reduce pyroptosis, and thus alleviating inflammation, suggesting that A20 may be a potent target in the treatment of periodontitis.

Keywords TNFAIP3 · Pyroptosis · Autophagy · Caspase-1 · Periodontitis

Introduction

Periodontitis is a polymicrobial infectious disease, which is caused by the disorder between host and microbe in the dental biofilm [1]. Periodontal bacteria could break down the balance of pro-inflammatory cytokines secretion, which aggravates the progression of inflammation in periodontal tissues [2]. Lipopolysaccharide (LPS) from *Porphyromonas gingivalis* (*P. gingivalis*) is considered as a key risk factor. It has been widely recognized that tobacco use is a non-negligible risk factor for periodontitis [3, 4]. Nicotine (NI), a major ingredient of cigarette, confuses the subgingival microflora and deteriorates the impairment in human periodontal tissues [5]. However, the mechanisms underlying the potential synergistic effect of NI and *Pg*.LPS on inflammation remains controversial.

Pyroptosis is a pivotal inflammatory form of programmed cell death (PCD), which is activated by inflammasomes [6]. It begins with the recognition of various pathogen stimuli, continues with cell swelling, membrane rupture, and DNA fragmentation, and finally ends with gasdermin D (GSDMD)-mediated pore formation on cell membranes along with inflammatory intracellular contents flowing out [7–9]. It is well established that cell death can exacerbate the penetration of pathogens and aggravate the development of the disease. Nod-like receptor protein 3 (NLRP3) inflammasome is currently the best reported inflammasome related to activation of caspase-1 and pyroptosis [10]. The critical role of pyroptosis in periodontitis has been reported. *T. denticola* surface protein, Td92, activated caspase-1, and pyroptosis in macrophages via NLRP3 inflammasome activation. And the Td92 has also

✉ Yan Xu
yanxu@njmu.edu.cn

[1] Jiangsu Key Laboratory of Oral Diseases, Nanjing Medical University, 1 # Shanghai Road, Nanjing, Jiangsu 210029, People's Republic of China

[2] Department of Periodontics, Affiliated Hospital of Stomatology, Nanjing Medical University, 1 # Shanghai Road, Nanjing, Jiangsu 210029, People's Republic of China

Table 1 Primers for real-time PCR

Gene	Forward primer	Reserve primer
GAPDH	5′-GTCTTCACCACCATGGAGAAG-3′	5′-GTTGTCATGGATGACCTTGGC-3′
IL-1β	5′-CAGCCAATCTTCATTGCTCA-3′	5′-TCGGAGATTCGTAGCTGGAT-3′
IL-6	5′-GTGCCTCTTTGCTGCTTTCAC-3′	5′-GGTACATCCTCGACGGCATCT-3′
TNF-α	5′-CACAGTGAAGTGCTGGCAAC-3′	5′-AGGAAGGCCTAAGGTCCACT-3′
IL-18	5′-TCGGGAAGAGGAAAGGAACC-3′	5′-TTCTACTGGTTCAGCAGCCA-3′

been reported to induce caspase-4-mediated pyroptosis by Cathepsin G in human gingival fibroblasts [11, 12]. *P. gingivalis* induced pyroptosis in both gingival fibroblasts and macrophage pyroptosis [13, 14]. Gasdermin E (GSDME) cleavage may trigger pyroptosis rather than GSDMD in human gingival epithelial cells [15]. In hPDLCs, the cyclic stretch could cause pyroptosis and induce inflammatory reaction through the cleavage of GSDMD [16].

Autophagy, a cellular mechanism participating in starvation adaptation, degradation of deserted proteins and organelles, tumor suppression, works as a "housekeeper" for the cellular homeostasis [17]. It has been reported that a close link existed between autophagy and periodontitis [18]. It is believed that autophagy could regulate redox which is an efficient and effective mechanism for antibacterial responses and protection against apoptosis. What's more, A20 (tumor necrosis factor-α-inducer protein 3, TNFAIP3) has also been reported to play an ambiguous role in autophagy. Inomata et al. [19] demonstrated that NDP52-mediated autophagy was inhibited by A20. A previous study has confirmed that A20 limits the induction of autophagy by reducing the ubiquitination of Beclin-1 [20]. However, another article reported a thoroughly opposing conclusion that A20 rescues the deficient autophagy in CD4 T cells [21].

A20, works as a regulator of ubiquitin, which tends to exert a negative effect on inflammation [22]. It has been further confirmed that loss of A20 could deteriorate human health. Patients carrying loss-of-function mutations of A20 may suffer from Behcet's disease, a chronic multisystemic inflammatory disease [23]. What's more, description from Parkinson's disease and multiple sclerosis shows the reduced A20 expression in peripheral blood is related to an elevated peripheral cytokines level such as interleukin (IL)-1β, IL-6, and tumor necrosis factor (TNF)-α) [24]. And it may account for the worrying condition compared with healthy subjects [25]. It also worked as a negative regulator of NLRP3 inflammasome activation to prevent Rheumatoid arthritis in vivo [26]. Significantly, the relationship between autophagy and pyroptosis has been highlighted. For instance, the suppression of Eukaryotic elongation factor-2 kinase restricted beclin-1-mediated autophagy and augmented pyroptosis in human melanoma cells [27]. Furthermore, acrolein-induced cell pyroptosis and suppressed cell migration by ROS-dependent autophagy [28]. In the present study, we hypothesized that A20 might prevent periodontitis by upregulating autophagy to alleviate inflammation and pyroptosis.

Fig. 1 *Pg*.LPS and NI induces NLRP3 inflammasome activation and pyroptosis. **a** Cells were cultured and stimulated with or without Z-YVAD-FMK ± *Pg*.LPS ± NI ± Nig. RT-PCR was performed to detect the mRNA of IL-1β, IL-6, IL-18, and TNF-α. **b** ELISA was performed for the detection of IL-1β, IL-6, IL-18, and TNF-α. **c** Western blot was performed to determine the levels of NLRP3, GSDMD, caspase-1, GSDMD-N, IL-1β, and IL-18. **d** The relative fold was target proteins to GAPDH. **e** The caspase-1 activity was evaluated in hPDLCs. **f** The cells were stained with Lyso-Tracker Red (red) and Hoechst 33,342 (blue) (Scale bar: 50 μm) **g** The LDH levels were measured with the LDH Cytotoxicity Assay Kit. **h** Photomicrographs of double-fluorescent staining with PI (red) and Calcein (green). (Scale bar: 200 μm) ($^{\#}P < 0.05$ vs. the CON group; $^{\#\#}P < 0.01$ vs. the CON group; $^{*}P < 0.05$ vs. the *Pg*.LPS + Nig group; $^{**}P < 0.01$ vs. the *Pg*.LPS + Nig group; $^{\$\$}P < 0.01$ vs. the *Pg*.LPS + NI + Nig group)

Materials and methods

Cell isolation and treatment

hPDLCs were cultured from periodontal ligament from healthy premolar teeth. These teeth were obtained from healthy donors aged between 11 and 18 years who underwent tooth extraction for orthodontic reasons. Every donor and corresponding guardian signed informed consent. The PDL fragments were gently separated from the middle third of the roots. hPDLCs were cultured in α minimum essential medium (Gibco, USA) supplemented 10% fetal bovine serum (Biological Industries, Israel) and 1% penicillin/streptomycin (Gibco, USA) then incubated at 37℃ in 5% CO_2. Cells between passage 3 and 5 were for all studies.

hPDLCs were exposed to *Pg*.LPS (1 μg/ml) (Invivogen, USA) plus NI (5 mM) (Sigma, USA) for 24 h prior to Nigericin (Nig) (10 μM) (MCE, USA) for 2 h for the induction of pyroptosis. To assess autophagic flux, cells were treated with bafilomycin A1 (BafA1, 200 nM for 6 h, Sigma, USA) to block the late phase of autophagy. This experiment involved pharmacological inhibitors or inducers. Cells were pre-treated with the addition of autophagy inhibitor 3-methyladenine (3MA, 5 mM for 24 h, Sigma, USA), autophagy inducer rapamycin (Rapa, 100 nM for 24 h, Selleck, USA),

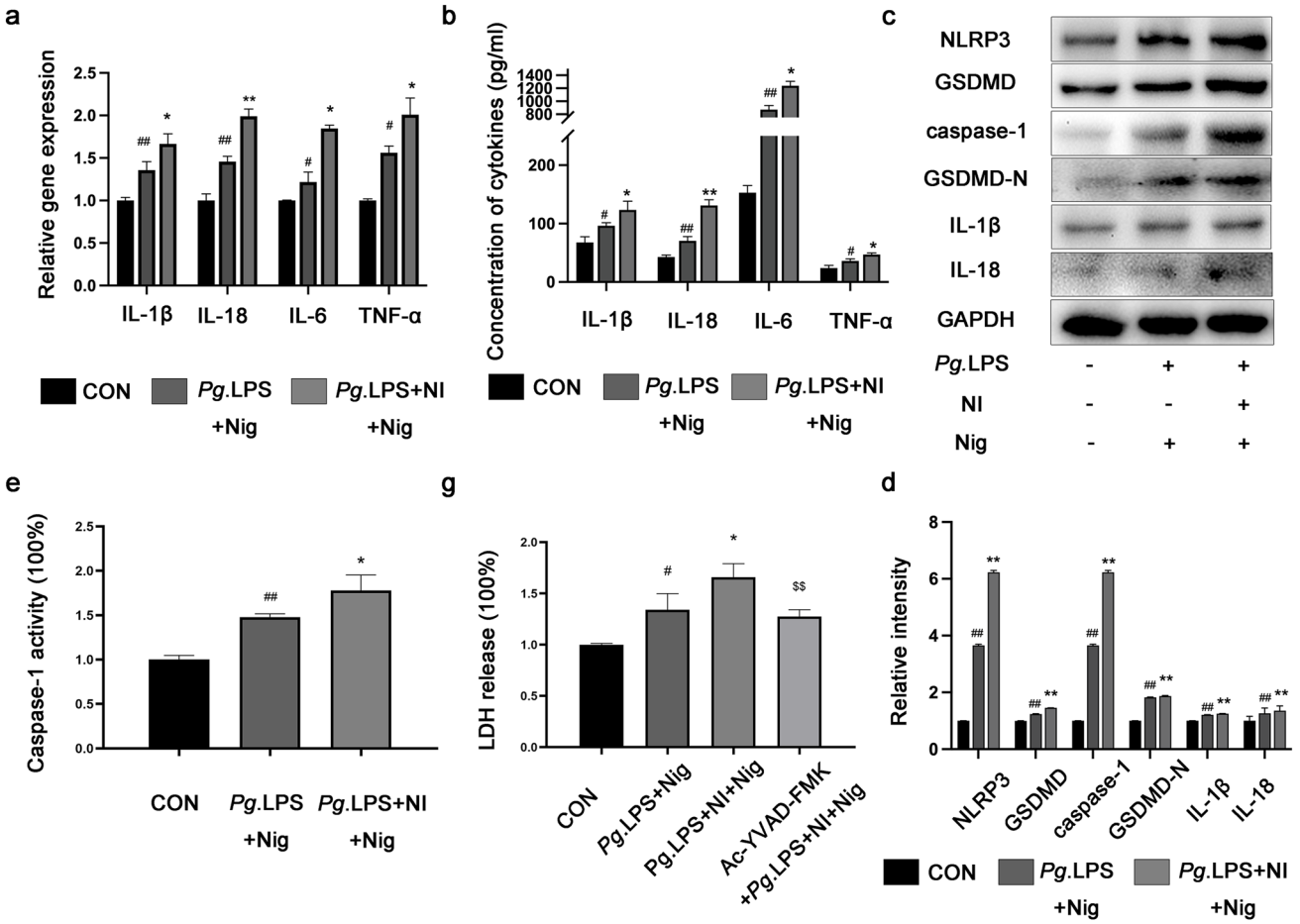
a
Relative gene expression
IL-1β
IL-18
IL-6
TNF-α
CON
Pg.LPS +Nig
Pg.LPS+NI +Nig
b
Concentration of cytokines (pg/ml)
c
NLRP3
GSDMD
caspase-1
GSDMD-N
IL-1β
IL-18
GAPDH
Pg.LPS
NI
Nig
e
Caspase-1 activity (100%)
g
LDH release (100%)
CON
Pg.LPS+Nig
Pg.LPS+NI+Nig
Ac-YVAD-FMK +Pg.LPS+NI+Nig
d
Relative intensity
f
Hoechst 33342
Lyso-Tracker Red
Merge
h
Calcein
PI
Merge
Ac-YVAD-FMK+ Pg.LPS+NI+Nig

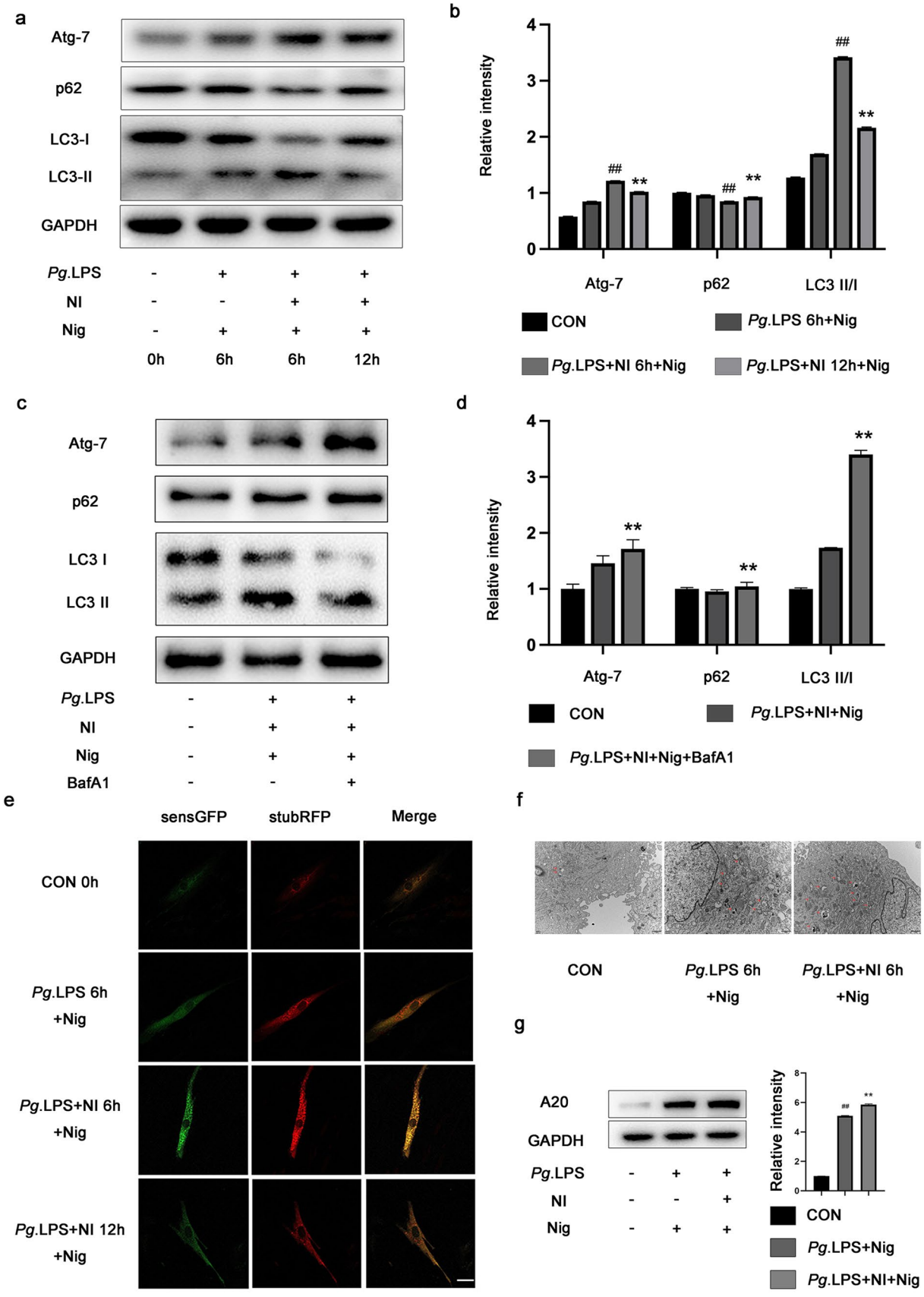
a
Atg-7
p62
LC3-I
LC3-II
GAPDH
Pg.LPS - + + +
NI - - + +
Nig - + + +
0h 6h 6h 12h
b
Relative intensity
Atg-7
p62
LC3 II/I
CON
Pg.LPS 6h+Nig
Pg.LPS+NI 6h+Nig
Pg.LPS+NI 12h+Nig
c
Atg-7
p62
LC3 I
LC3 II
GAPDH
Pg.LPS - + +
NI - + +
Nig - + +
BafA1 - - +
d
Relative intensity
Atg-7
p62
LC3 II/I
CON
Pg.LPS+NI+Nig
Pg.LPS+NI+Nig+BafA1
e
sensGFP
stubRFP
Merge
CON 0h
Pg.LPS 6h +Nig
Pg.LPS+NI 6h +Nig
Pg.LPS+NI 12h +Nig
f
CON
Pg.LPS 6h +Nig
Pg.LPS+NI 6h +Nig
g
A20
GAPDH
Pg.LPS - + +
NI - - +
Nig - + +
Relative intensity
CON
Pg.LPS+Nig
Pg.LPS+NI+Nig

◂**Fig. 2** *Pg*.LPS and NI exposure led to an upregulation of autophagy at 6 h. Cells were stimulated with or without *Pg*.LPS ± NI ± Nig. **a–c** The levels of Atg-7, p62, LC3-II/I were measured by Western blot. **b–d** Quantitative analysis of these proteins related to GAPDH were shown in the bar graph. **e** Cells were transfected with the stubRFP-sensGFP-LC3 Lentivirus to monitor the autophagic flux and examined by confocal microscope. (Scale bar: 200 μm) ($n=4$) **f** Ultrastructural features of hPDLCs by TEM. (Scale bar: 200 nm and 1 μm) **g** Western blot was performed to determine the expression of A20. Relative expression of A20/GAPDH was analyzed. ($^{\#\#}P<0.01$ vs. the CON group; $^{**}P<0.01$ vs. the *Pg*.LPS + NI 6 h group)

and caspase-1 inhibitor Z-YVAD-FMK (10 μM for 24 h, MCE, USA), thereafter the cells were washed with PBS twice for the following treatment as stated.

Immunocytochemistry (ICC)

Cells were washed with PBS and fixed with 4% paraformaldehyde for 15 min, then incubated with 0.5% Triton-100 at room temperature for 20 min, and washed with PBS. The cells were blocked with 3% BSA for 30 min. After discarding the blocking solution, diluted primary antibody against vimentin (1:200, Servicebio) or keratin (1:200, Servicebio) was applied to the slides overnight at 4 °C in the wet box. And then the slides were washed with PBS and incubated with secondary antibody at room temperature for 50 min. Horseradish peroxidase-conjugated avidin was added, and the cells were incubated at 37 °C for 20 min. And being washed with PBS, slides were stained with DAB and counterstained with hematoxylin. The samples were dehydrated and sealed. Images were photographed with a Leica fluorescence microscope.

Real-time quantitative PCR (RT-PCR)

Total mRNA was isolated with RNA Extraction Kit (TaKaRa, Japan) according to the manufacturer's protocol. cDNA was synthesized by PrimeScript RT Master Mix (TaKaRa, Japan). The RT-PCR was performed with SYBR Premix Ex Taq II in a 10 μl reaction system (TaKaRa, Japan). Reactions were performed on an ABI7900 apparatus. Primers are described in Table 1.

Enzyme-linked immunosorbent assay (ELISA)

After the respective incubation periods, IL-1β, IL-18, TNF-α, and IL-6 levels in the culture supernatants were measured with human ELISA kits (Neobioscience, China) according to the manufacturer's instructions.

Western blotting analysis

Proteins were extracted from hPDLCs in six-well plates with different treatments. Total protein was prepared with cell lysates (Beyotime, China). After protein separating with 10–12% SDS–PAGE, it transferred to PVDF membranes. The membranes were sealed with 5% skimmed milk for 2 h at room temperature. Subsequently, the protein were incubated with diluted primary antibodies targeting at NLRP3 (1:1000, CST), GSDMD (1:1000, Abcam), caspase-1 (1:1000,CST), IL-1β (1:1000, CST), GSDMD-N (1:1000, Abcam), IL-18 (1:1000, Abcam), Atg-7 (1:100,000, Abcam), p62 (1:1000, Abcam),LC 3B (1:2000, Abcam), and GAPDH (1:1000) overnight at 4℃. Then, the membrane was rinsed with TBST three times and secondary antibody (1:8000) was applied for 60 min. An Enhanced Chemiluminescence Detection Kit (Millipore, Germany) was used for immunodetection.

Caspase-1 activity

The Z-WEHD-luminescent caspase-1 substrate solution is reconstituted at room temperature [29]. Then resultant solution is combined 1:1 with the prepared sample in the 96-well plate. The mixed were incubated for 1.5 h for the stable luminescent signal, according to the manufacturer instruction (Promega, USA). All luminescence was recorded on a luminescence plate reader.

Lyso-Tracker Red (LTR) staining

To detect the integrity of lysosomal membrane, we adopt LTR staining (Beyotime, China). After being stimulated, cells were incubated with LTR working solution for 30 min and Hoechst 33,342 for 5 min at 37 ℃ and washed for three times with PBS. Images were photographed with a Leica fluorescence microscope.

Calcein/propidium iodide (PI) staining

hPDLCs were stained Calcein/PI with the assay from Beyotime. After different stimulation, the cells were incubated with Calcein/PI working solution for 30 min at 37 °C in the dark and washed three times with PBS. The images of samples were acquired by a Leica fluorescence microscope.

Lactate dehydrogenase (LDH) release assay

hPDLCs were treated with the described experimental designs. The amount of LDH release was determined by a commercial LDH assay kit (Beyotime, China) following the manufacturer's instructions.

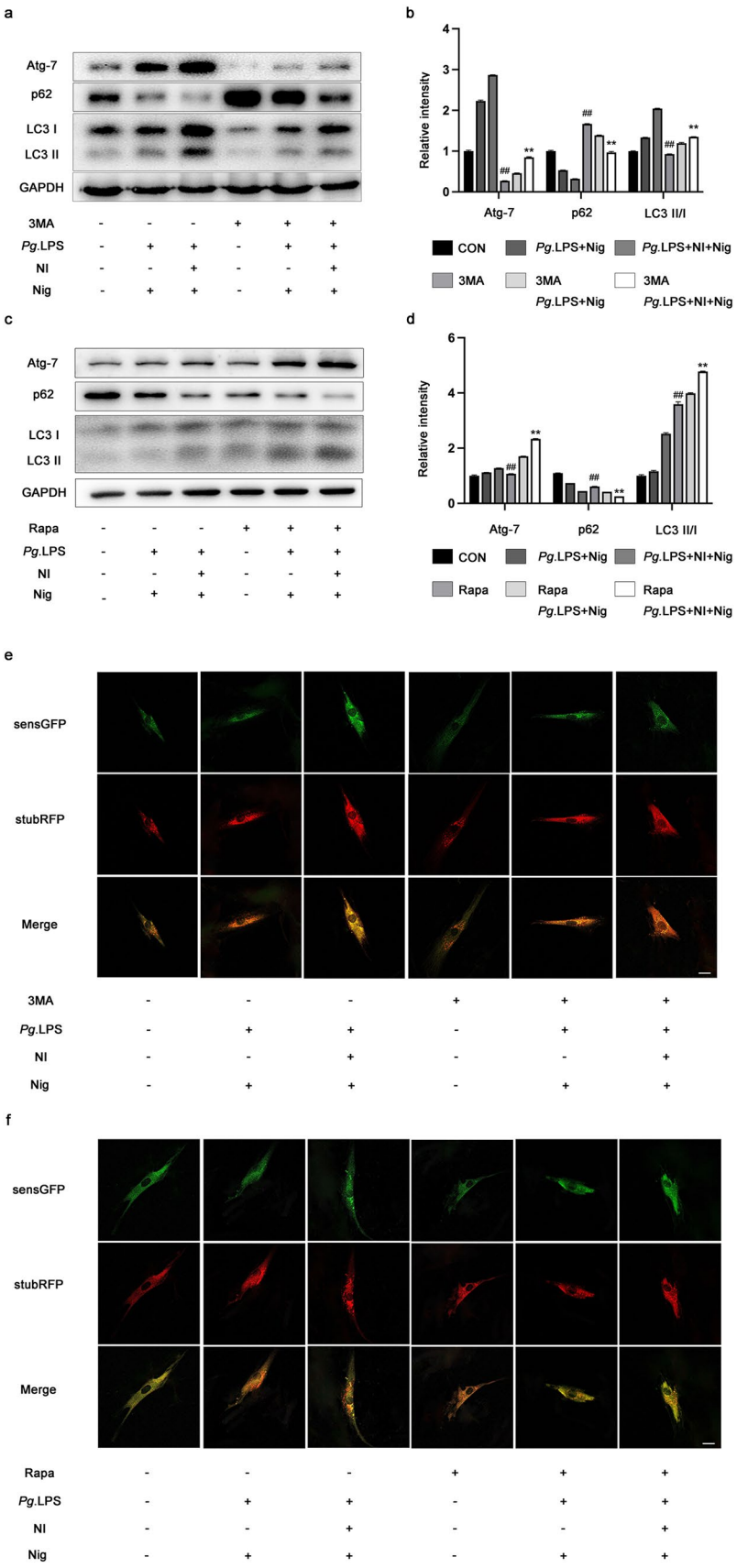

Fig. 3 3MA inhibits autophagy and Rapa enhanced it in hPDLCs stimulated by *Pg*. LPS and NI. Cells were stimulated with or without 3MA ± Rapa ± *Pg*. LPS ± NI ± Nig. **a**–**c** Western blot was used to detect the levels of Atg-7, p62, LC3-II/I. **b**–**d** The relative fold was target proteins to GAPDH. **e**, **f** Cells were initially transfected with the stubRFP-sensGFP-LC3 Lentivirus, and examined by confocal microscope. (Scale bar: 200 μm) ($^{\#\#}P < 0.01$ vs. the CON group; $^{**}P < 0.01$ vs. the *Pg*.LPS)

Autophagy detection

To assess the autophagic flux status, hPDLCs were transfected with StubRFP-SensGFP-LC3 lentivirus (Genechem, China) for 12 h. The red/green co-localized puncta indicate the formation of autophagosomes (yellow punctuation). When the green fluorescence is quenched, only red single fluorescent punctate clusters can be detected, which indicates the formation of autophagic lysosomes. hPDLCs were plated in a 12-well dish, transfected with lentivirus for 12 h, and challenged with different stimulation. The LC3-labeled puncta pattern was observed by a laser-scanning confocal microscope (Leica, Germany).

Transmission electron microscopy (TEM)

Pre-treated cells were harvested to measure autophagosomes by TEM (Tokyo, Japan). They were fixed with 2.5% glutaraldehyde overnight at 4 °C, and subsequently post-fixed in 1% OsO_4 at room temperature for 2 h. The samples were dehydrated with ethanol series and embedded in epoxy resin. Next, the ultrathin sections were excised and stained with uranyl acetate and lead citrate.

Lentivirus preparation and infection

After transfecting hPDLCs with lentivirus A20 (GenePharma, China) for overexpression or silencing studies, the positive cells were selected with puromycin (2.5 μg/mL, 12 h). The infection efficiency was over 80%**.**

Statistical analysis

Data were extracted from three independent experiments unless noted otherwise. Each value is represented as the mean ± SD. When the data are in a normal distribution, differences among groups were evaluated, using the Student *t* test of two independent samples and one-way ANOVA of three or more independent samples. When P value < 0.05 the data were considered statistically significant.

Results

Identification of hPDLCs

The primary hPDLCs cultured by the tissue block method could be seen after 5–7 days, crawling from the of the tissue block radially (Fig. S1a). Since vimentin is the marker of fibroblast and keratin is mainly present in epithelial cells, we applied these two markers to identify the primary hPDLCs. The ICC showed the presence of vimentin and absence of keratin in the cytoplasm (Fig. S1b, c) indicating that they were mesenchymal cells rather epithelial cell.

NLRP3 inflammasome activation and caspase-1-mediated pyroptosis were induced in hPDLCs

The overactivation of NLRP3 inflammasome may trigger pyroptosis and the release of inflammatory cytokines. As indicated in Fig. 1a, *Pg*.LPS plus Nig significantly increased the expression of IL-1β, IL-18, IL-6, TNF-α, and the combination of *Pg*.LPS, NI and Nig further enhanced the mRNA level of these pro-inflammatory cytokines mentioned above. Consistently, similar changes of IL-1β, IL-18, IL-6, and TNF-α in the culture supernatants were obtained by ELISA (Fig. 1b). To detect the NLRP3 inflammasome activation and subsequent pyroptosis, the protein expression level of NLRP3, GSDMD, caspase-1, GSDMD-N, IL-1β, and IL-18 were measured. As shown in Fig. 1c, d, stimulated with *Pg*.LPS plus Nig, the pyroptotic proteins expression were significantly increased compared with CON group. And *Pg*.LPS, NI along with Nig enhanced the related proteins expression as mentioned above (Fig. 1c, d). We further detected the caspase-1 activity. As shown in Fig. 1e, *Pg*.LPS plus Nig increased the caspase-1 activity and the co-stimulation of *Pg*.LPS, NI and Nig further intensified it. To detect the lysosome function, LTR was applied to visualized lysosomes in live cells. Treatment with *Pg*.LPS, NI and Nig markedly reduced the fluorescence intensity (Fig. 1f and S2a). The collective data indicate the activation of NLRP3 inflammasome in *Pg*.LPS-, NI-, and Nig-treated hPDLCs. *Pg*.LPS-, NI-, and Nig-treated cells were counterstained with Calcein/PI, while PI-positive indicated the cell membrane integrity was destroyed and dead cells. We also detected the release of LDH as a marker of pyroptosis. As shown in Fig. 1g, h and S2b, *Pg*.LPS-, NI-, and Nig-induced pore formation and membrane rupture, as indicated by the increased LDH activity and the PI-positive staining cells and pretreatment of Z-YVAD-FMK (the caspase-1 inhibitor) reversed them. Together, these results suggest that *Pg*.LPS, NI and Nig may induce pyroptosis in hPDLCs.

A20 modulated autophagy in hPDLCs

To monitor the autophagic flux in hPDLCs, cells were treated with *Pg*.LPS plus NI for 0, 6, and 12 h in prior to Nig. As shown in Fig. 2a, b, the ratio of LC3-II/LC3-I and the level of Atg-7 were increased at 6 h and then decreased at 12 h, whereas the expression of p62 decreased at 6 h and then increased at 12 h. Taken together, *Pg*.LPS, NI, and Nig exposure led to a dramatic upregulation of autophagy at 6 h. Next, autophagy flux was further

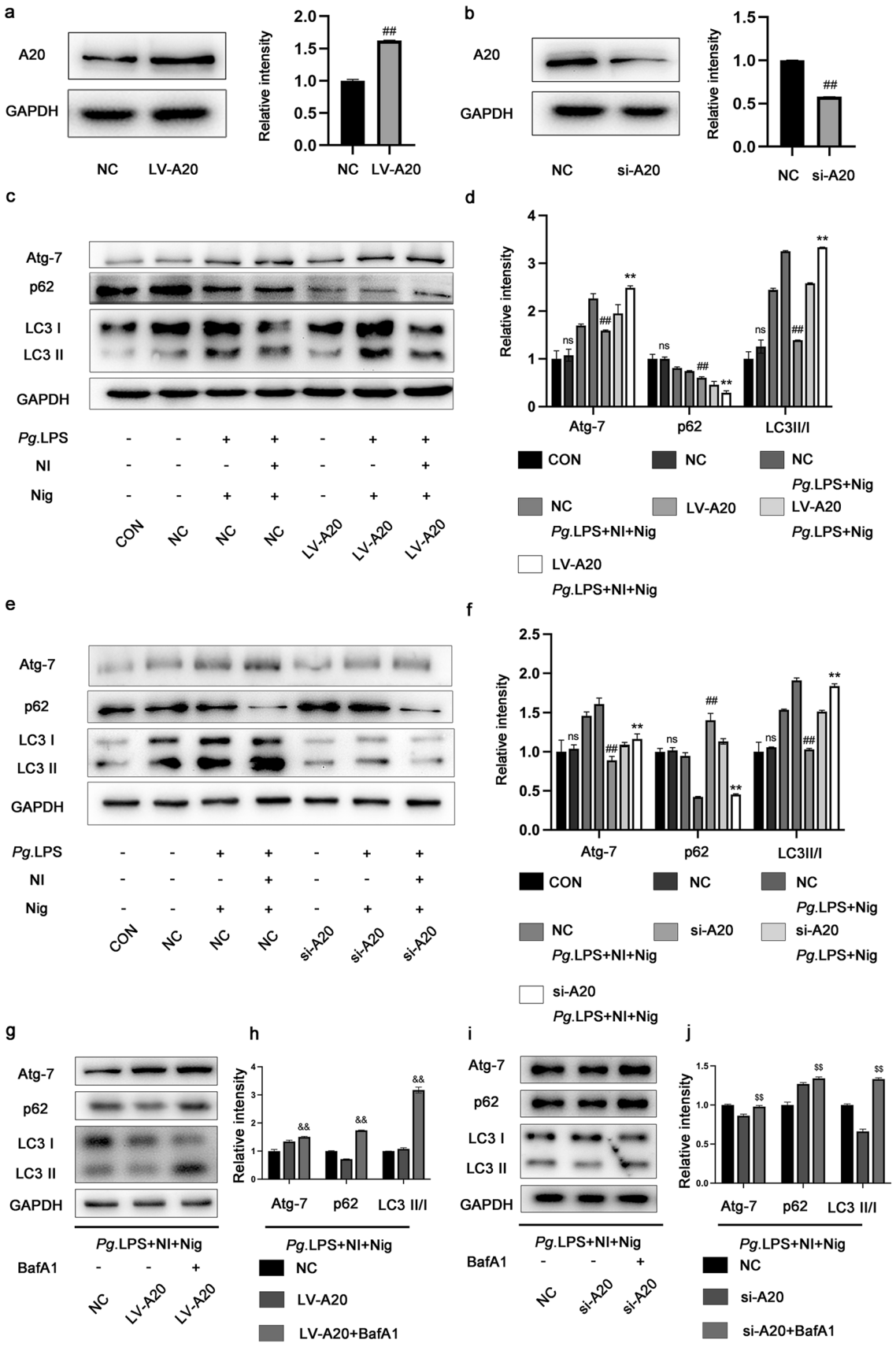
a
A20
GAPDH
NC LV-A20
Relative intensity
NC LV-A20
b
A20
GAPDH
NC si-A20
Relative intensity
NC si-A20
c
Atg-7
p62
LC3 I
LC3 II
GAPDH
Pg.LPS
NI
Nig
CON NC NC NC LV-A20 LV-A20 LV-A20
d
Relative intensity
Atg-7 p62 LC3II/I
CON
NC
NC Pg.LPS+Nig
NC Pg.LPS+NI+Nig
LV-A20
LV-A20 Pg.LPS+Nig
LV-A20 Pg.LPS+NI+Nig
e
Atg-7
p62
LC3 I
LC3 II
GAPDH
Pg.LPS
NI
Nig
CON NC NC NC si-A20 si-A20 si-A20
f
Relative intensity
Atg-7 p62 LC3II/I
CON
NC
NC Pg.LPS+Nig
NC Pg.LPS+NI+Nig
si-A20
si-A20 Pg.LPS+Nig
si-A20 Pg.LPS+NI+Nig
g
Atg-7
p62
LC3 I
LC3 II
GAPDH
Pg.LPS+NI+Nig
BafA1
NC LV-A20 LV-A20
h
Relative intensity
Atg-7 p62 LC3 II/I
Pg.LPS+NI+Nig
NC
LV-A20
LV-A20+BafA1
i
Atg-7
p62
LC3 I
LC3 II
GAPDH
Pg.LPS+NI+Nig
BafA1
NC si-A20 si-A20
j
Relative intensity
Atg-7 p62 LC3 II/I
Pg.LPS+NI+Nig
NC
si-A20
si-A20+BafA1

◂**Fig. 4** A20 modulated autophagy in hPDLCs stimulated with *Pg*. LPS and NI. **a** Upregulation or **b** Downregulation of A20 was detected by western blot with quantitative analysis in NC-, LV-A20- or si-A20-infected cells. Cells were stimulated with or without *Pg*. LPS ± NI ± Nig ± BafA1. **c**, **g** In NC and LV-A20 groups, the levels of Atg-7, p62, LC3-II/I were measured by Western blot. **d**, **h** Quantitation was performed of target proteins and the expression of GAPDH was used as an internal control. **e**, **i** Atg-7, p62, LC3-II/I expression was detected by western blot **f**, **j** with quantitative analysis when cells transfected with NC or si-A20. (ns $P > 0.05$ vs. the CON group; $^{\#\#}P < 0.01$ vs. the NC group; $^{**}P < 0.01$ vs. the NC *Pg*. LPS + NI + Nig; $^{\&\&}P < 0.01$ vs. LV-A20 group; $^{\$\$}P < 0.01$ vs. si-A20 group)

detected by BafA1, an inhibitor of autophagosome–lysosome fusion. *Pg*.LPS, NI and Nig exposure led to further increase of Atg-7 and LC3-II/I level in the presence of BafA1, suggesting that autophagy flux level was increased (Fig. 2c, d). Also, BafA1 treatment led to a similar strong accumulation of p62 (Fig. 2c, d). Confocal microscopic images depicted that hPDLCs transfected with StubRFP-SensGFP-LC3 lentivirus incubation of *Pg*.LPS, NI, and Nig for 6 h significantly increased red/green co-localized dot-like aggregation, which was consistent with the results of autophagy-related proteins (Fig. 2e). The autophagic ultrastructure was examined by TEM. An accumulation of autophagosomes was detected in *Pg*.LPS-, NI-, and Nig-treated hPDLCs by TEM compared with CON group (Fig. 2f). We detected A20 expressions under different stimuli to verify that A20 may tend to exert a regulatory effect in autophagy. A20 protein levels were significantly increased after the stimulation of *Pg*.LPS and Nig. NI further increased A20 expression (Fig. 2g).

Autophagy inhibitor 3MA and autophagy inducer Rapa were applied. As shown in Fig. 3a, b, the protein levels Atg-7, and LC3-II/LC3-I were decreased by 3MA-pretreatment, while p62 expression was increased. In contrast, Rapa-pretreatment showed the opposite results (Fig. 3c, d). Also, the number of red/green co-localized dot-like aggregation were increased by Rapa and decreased by 3MA (Fig. 3e, f). To explore the role of A20 in *Pg*.LPS-, NI-, and Nig-induced autophagy, lentivirus targeting A20 were applied. As shown in Fig. 4a, b, the protein level of A20 was increased/decreased in the LV-A20/si-A20 group. In the LV-A20 group, the expression of Atg-7 and LC3-II/LC3-I increased, whereas the p62 expression decreased (Fig. 4c, d). In contrast, A20 knockdown accelerated the inhibition of endogenous LC3-I to LC3-II conversion and the autophagy-related protein Atg-7 and Beclin-1. Conversely, the p62 secretion was highly reduced (Fig. 4e, f). Similarly, BafA1 treatment led to accumulation of Atg-7, p62 and LC3BII/LC3BI ratio in both LV-A20 and si-A20 group (Fig. 4g, h).

Autophagy negatively regulates pyroptosis in hPDLCs stimulated by Pg.LPS and NI

To explore the role autophagy on pyroptosis, 3MA and Rapa were applied. Pre-treated with 3MA enhanced the secretion of the inflammatory cytokines, whereas Rapa diminished it (Fig. 5a, b). As shown in Fig. 5c, d, the protein level of NLRP3, caspase-1, IL-1β, IL-18, GSDMD, and GSDMD-N were further increased in *Pg*.LPS-, NI-, and Nig-induced-cells pre-treated by 3MA. Rapa decreased the related proteins expression (Fig. 5e, f). Also, similar trends were detected in the results of caspase-1 activity (Fig. 5g). The fluorescence intensity of LTR was abolished by 3MA and aggravated by Rapa (Fig. 5h and S2c). The role of autophagy on pyroptosis was deeply assessed by LDH release and Calcein-AM/PI Staining, the LDH release and PI-positive cells were elevated by 3MA and suppressed by Rapa (Fig. 5i, j and S2d). The data above implied that autophagy may negatively regulate pyroptosis in hPDLCs.

A20 modulates the activation of NLRP3 inflammasome and pyroptosis by autophagy in hPDLCs

To verify the potential mechanism underlying this process, hPDLCs were transfected with lentivirus targeting A20. Rapa and 3MA were also applied to explore the role of autophagy in the A20-related activation of NLRP3 inflammasome and pyroptosis. In Fig. 6a–d, A20 upregulation decreased the IL-1β, IL-18, IL-6, and TNF-α secretion attenuating inflammation, nevertheless, si-A20 increased the trend. When pre-treated with 3MA or Rapa, the secretion of cytokines was further enhanced or inhibited. In the LV-A20 group, the protein levels of NLRP3, caspase-1, IL-1β, IL-18, GSDMD, and GSDMD-N were rescued, and they were enhanced or diminished by 3MA or Rapa (Fig. 6e, f). As shown in Fig. 6g, h, NLRP3, caspase-1, IL-1β, IL-18, GSDMD, and GSDMD-N expression were increased in si-A20 group. And 3MA and Rapa showed similar results in A20 silencing cells. Accordingly, the decrease/increase of caspase-1 activity in the LV-A20 or si-A20 group showed that expression of A20 was responsible for it. The caspase-1 activity could be reversed by Rapa or aggravated by 3MA in both the LV-A20 group and si-A20 group (Fig. 6i, j). Simultaneously, the decrease fluorescence intensity of LTR was reversed by the overexpression of A20, which could be further intensified by the Rapa or attenuated by 3MA (Fig. 6k and S2e). In Fig. 6l and S2f, the fluorescence of LTR was darkened when A20 was knockdown. Identically, 3MA and Rapa showed the same effect in the si-A20 group. Furthermore, the results

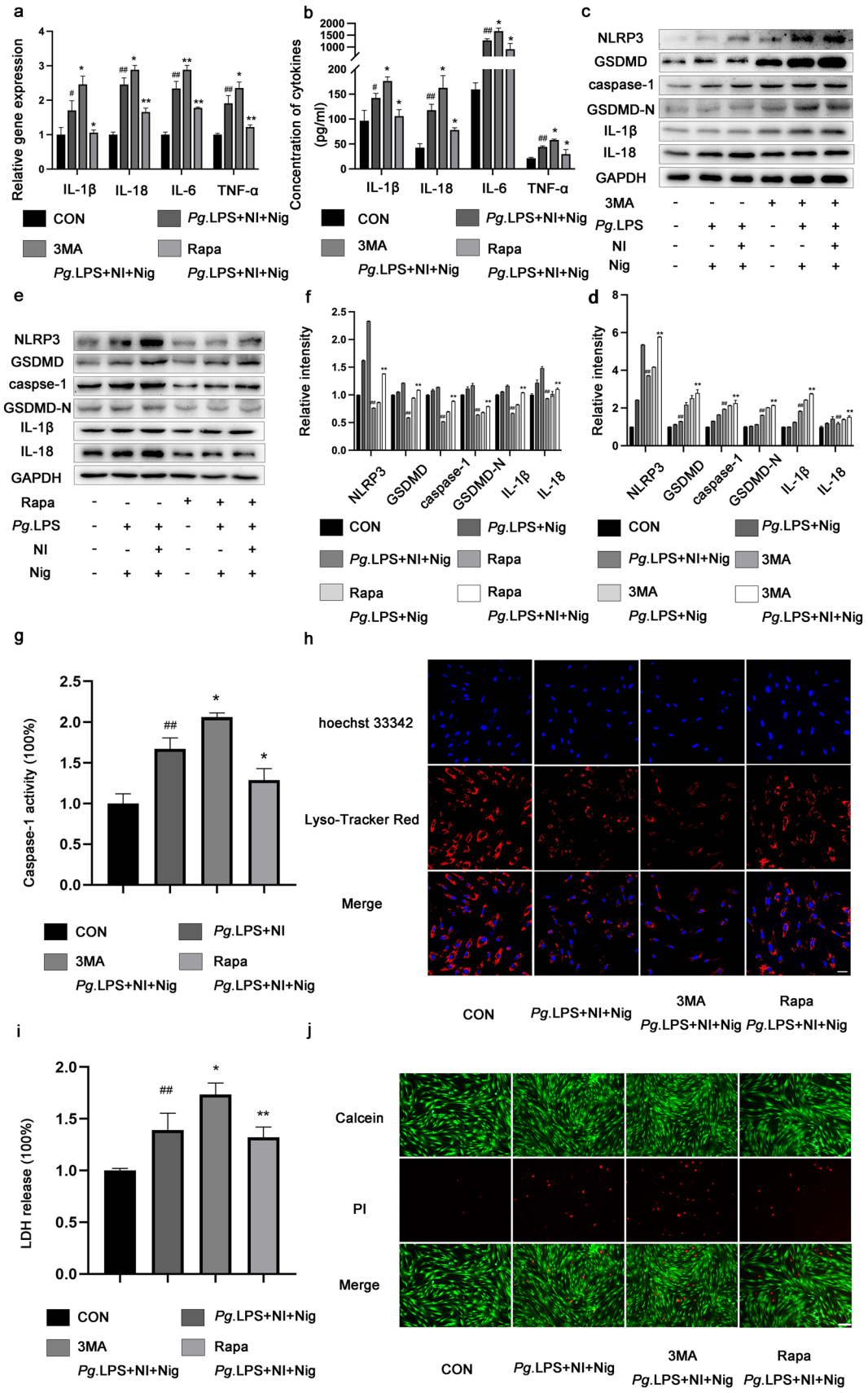
a
Relative gene expression
IL-1β
IL-18
IL-6
TNF-α
CON
Pg.LPS+NI+Nig
3MA
Pg.LPS+NI+Nig
Rapa
Pg.LPS+NI+Nig
b
Concentration of cytokines (pg/ml)
IL-1β
IL-18
IL-6
TNF-α
CON
Pg.LPS+NI+Nig
3MA
Pg.LPS+NI+Nig
Rapa
Pg.LPS+NI+Nig
c
NLRP3
GSDMD
caspase-1
GSDMD-N
IL-1β
IL-18
GAPDH
3MA
Pg.LPS
NI
Nig
e
NLRP3
GSDMD
caspse-1
GSDMD-N
IL-1β
IL-18
GAPDH
Rapa
Pg.LPS
NI
Nig
f
Relative intensity
NLRP3
GSDMD
caspase-1
GSDMD-N
IL-1β
IL-18
CON
Pg.LPS+Nig
Pg.LPS+NI+Nig
Rapa
Rapa
Pg.LPS+Nig
Rapa
Pg.LPS+NI+Nig
d
Relative intensity
NLRP3
GSDMD
caspase-1
GSDMD-N
IL-1β
IL-18
CON
Pg.LPS+Nig
Pg.LPS+NI+Nig
3MA
3MA
Pg.LPS+Nig
3MA
Pg.LPS+NI+Nig
g
Caspase-1 activity (100%)
CON
Pg.LPS+NI
3MA
Pg.LPS+NI+Nig
Rapa
Pg.LPS+NI+Nig
h
hoechst 33342
Lyso-Tracker Red
Merge
CON
Pg.LPS+NI+Nig
3MA
Pg.LPS+NI+Nig
Rapa
Pg.LPS+NI+Nig
i
LDH release (100%)
CON
Pg.LPS+NI+Nig
3MA
Pg.LPS+NI+Nig
Rapa
Pg.LPS+NI+Nig
j
Calcein
PI
Merge
CON
Pg.LPS+NI+Nig
3MA
Pg.LPS+NI+Nig
Rapa
Pg.LPS+NI+Nig

◂**Fig. 5** Autophagy negatively regulates pyroptosis in hPDLCs stimulated by *Pg*.LPS and NI. Cells were pre-treated with or without 3MA or Rapa, and then treated with *Pg*.LPS ± NI ± Nig. **a** RT-PCR was performed to detect the mRNA expressions of IL-1β, IL-18, IL-6, and TNF-α. **b** ELISA was performed for IL-1β, IL-18, IL-6, and TNF-α in the supernatants. **c**, **e** Western blot was used to detect the levels of NLRP3, GSDMD, caspase-1, GSDMD-N, IL-1β, and IL-18. **d**, **f** Quantitative analysis of these proteins related to GAPDH were shown in the bar graph. **g** The relative luminescence results of caspase-1 were recorded. **h** The cells were stained with Lyso-Tracker Red (red) and Hoechst 33,342 (blue). (Scale bar: 50 μm) **i** The LDH levels were measured by the LDH Cytotoxicity Assay Kit. **j** Cells were double-stained with PI (red) and Calcein (green). (Scale bar: 200 μm) ($^{\#}P < 0.05$ vs. the CON group; $^{\#\#}P < 0.01$ vs. the CON group; $^{*}P < 0.05$ vs. the *Pg*.LPS group; $^{**}P < 0.01$ vs. the *Pg*.LPS group)

of LDH release and PI staining showed similar results (Fig. 6m–p and S2g, h). The collective data above determined that A20 modulated activation of NLRP3 inflammasome and pyroptosis by activating autophagy.

Discussion

Periodontal tissue is damaged when the balance between inflammatory responses and host immunity is ruined. The use of tobacco is one of the system risk factors for periodontal disease. NI, the main component of a cigarette, exacerbated pathological changes in human periodontal tissue. This study demonstrated that *Pg*.LPS- and NI-induced the NLRP3 inflammasome activation and subsequent pyroptosis in hPDLCs. *Pg*.LPS and NI exposure led to a dramatic upregulation of autophagy at 6 h. Furthermore, A20 inhibited NI- and *Pg*. LPS-induced NLRP3 inflammasome activation and pyroptotic death of hPDLCs by promoting cell autophagy (Fig. 7). These results were verified by the pretreatment of 3MA or Rapa.

The activation transcription factor nuclear factor-κB (NF-κB) plays a positive role in the progression of many inflammatory diseases. A20, as a negative regulator of NF-κB signaling, exerts an anti-inflammatory effect [30]. Besides, an inverse correlation between the incidence of type 2 diabetes and A20 mRNA levels was found [31]. In our study, evidence revealed that A20 protein levels were significantly increased by *Pg*.LPS. The co-stimulation further increased A20 expression. Under the challenge of *Pg*.LPS and NI, the corresponding elevating A20 secretion tends to inhibit inflammatory response. The present data showed that increased A20 expression led to restricted secretion of inflammatory cytokines (IL-6 and TNF-α).

Pyroptosis is a kind of PCD characterized by membrane pore formation, cell swelling, and membrane rupture, as well as the release of inflammatory cytokines. The NLRP3 inflammasome, a multiprotein complex, could be activated upon pathogen and stress [32, 33]. Pyroptosis is triggered by caspase-1 after activation of NLRP3 inflammasomes. Caspase-1 plays sufficient roles in initiating pyroptosis, which is a protease cleaving target protein. Furthermore, different from other apoptotic caspases, caspase-1 is well-known as the inflammatory caspase, which could produce IL-1β [34]. Walle LV et al. [26] have reported that A20 may exert a negative effect on the activation of NLRP3 inflammasome, by targeting at NF-κB signaling pathway. Stimulated by diverse stimuli, such as pathogen-associated molecular patterns (PAMPs) or damage-associated molecular patterns (DAMPs), the expression NLRP3 and pro-IL-1β upregulates through translocation of NF-κB, and the microbial products or endogenous signals trigger ROS activation, mitochondrial dysfunction, or lysosome permeabilization. Under these stimuli, the protein components of NLRP3 inflammasome aggregate to activate NLRP3 inflammasome, and express mature caspase-1 and IL-1β [10]. Furthermore, IL-1β, the inducer of inflammation, increases during the pathogenesis of periodontitis. The damage of periodontal tissue, such as the clinical attachment loss and alveolar bone loss, may arise from the upregulating IL-1β activity [35]. Gasdermin D is one of six gasdermin family members in human, which could be cleaved by caspase-1. And then the cleavage of GSDMD releases the N-terminal fragment of GSDMD. The N-terminal fragment of GSDMD could form plasma membrane pores, leading to the induction of pyroptotic activity [36]. Our study verified that *Pg*.LPS and NI increased the expression of NLRP3, GSDMD, caspase-1 and IL-1β in hPDLCs, and the overexpression of A20 suppressed pyroptosis in *Pg*.LPS- and NI-exposed cells.

Autophagy is a cellular pathway for degrading damaged proteins and removing the invading bacteria. It is characterized by increased expression levels of specific proteins, such as LC3-II/LC3-I ratio, Beclin-1, and Atg-7, and decreased expression levels of p62. It has been reported that poly(I:C) stimulation induces NDP52-mediated autophagy and A20 plays an important counter-regulatory role in it [19]. A20 may also react with the mechanistic target of rapamycin (mTOR) and restricts mTOR activity, resulting in amplified autophagy in CD4 T cells [21]. The deubiquitinating enzyme A20 reduced the ubiquitination of Beclin-1 and then restricted autophagy in response to Toll-like receptor (TLR) signaling during inflammatory responses [20]. A20 may play a non-negligible role in the modulation of autophagy. The dysregulation of autophagy has been implicated in oral diseases including periapical lesions, oral cancer, and periodontitis. It has been presumed that autophagy can facilitate cellular homeostasis against external stressors in an early stage. But in the late stage, it promotes cell death through the Akt/mTOR/survivin signaling pathway in the pathogenesis of periapical lesions [37]. Decreased

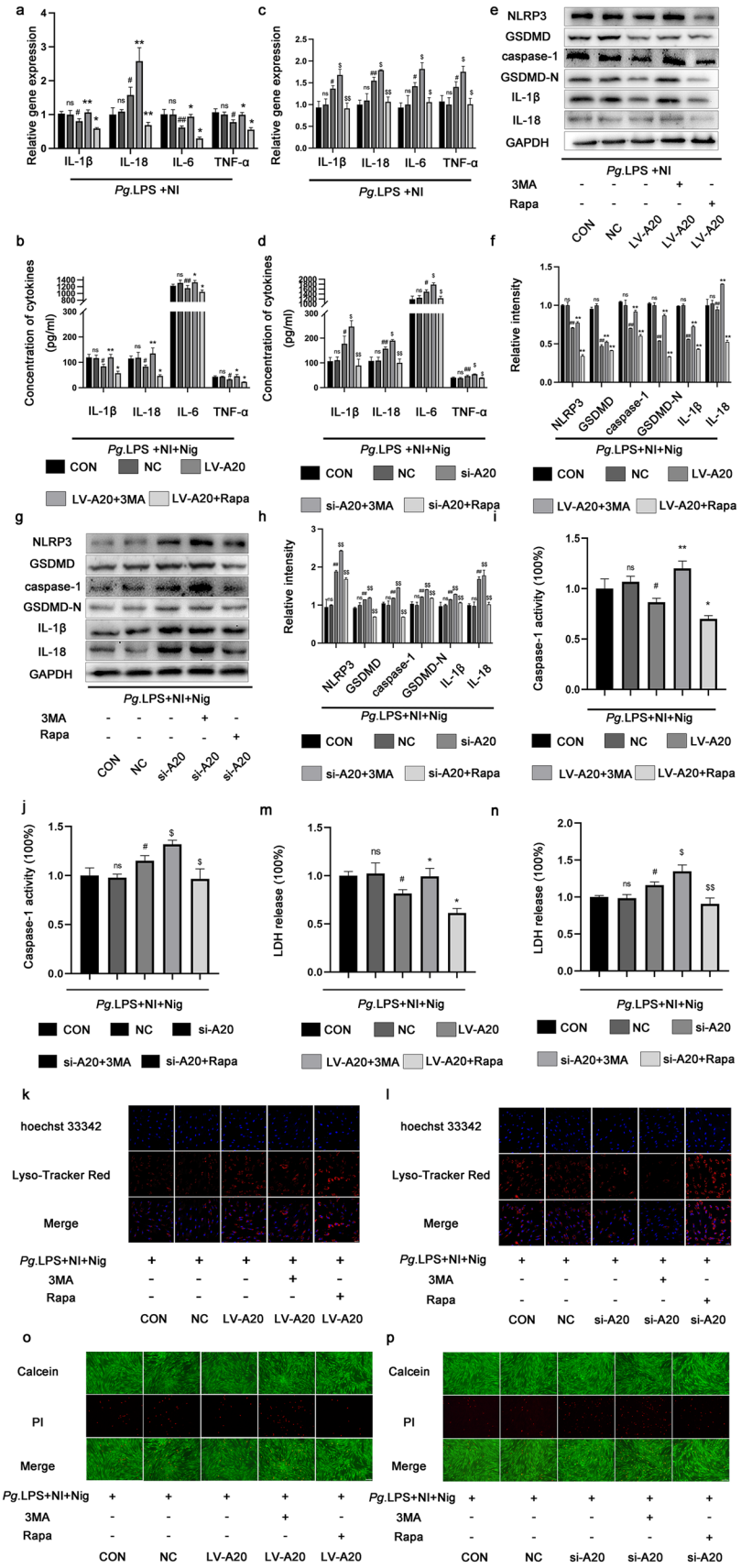

Fig. 6 A20 modulates the activation of NLRP3 inflammasome and pyroptosis by autophagy in *Pg*.LPS and NI-induced hPDLCs. Cells were infected with LV-A20, si-A20 or NC lentivirus, and then pre-treated with or without 3MA ± Rapa ± *Pg*.LPS ± NI ± Nig. The expressions of IL-1β, IL-18, IL-6 and TNF-α in cells infected with LV-A20 lentivirus were detected by **a** RT-PCR and **b** ELISA. The expression of IL-1β, IL-18, IL-6, and TNF-α in cells infected with si-A20 lentivirus were detected by **c** RT-PCR and **d** ELISA. **e**, **g** Western blot was used to detect the levels of NLRP3, GSDMD, caspase-1, GSDMD-N, IL-1β, and IL-18. **f**, **h** Relative expression of these proteins was expressed as a percentage of GAPDH. **i**, **j** The relative caspase-1 activity was detected by caspase-1 activity assay. **k**, **l** The cells were stained with Lyso-Tracker Red (red) and Hoechst 33,342 (blue). (Scale bar:50 μm) **m**, **n** The LDH levels were measured by the LDH Cytotoxicity Assay Kit. **o**, **p** Cells were double-stained with PI (red) and Calcein (green). (Scale bar: 200 μm) (ns $P > 0.05$ vs. the CON group; $^{\#}P < 0.05$ vs. the NC group; $^{\#\#}P < 0.01$ vs. the NC group; $^{*}P < 0.05$ vs. the LV-A20 group; $^{**}P < 0.01$ vs. the LV-A20 group; $^{\$}P < 0.05$ vs. the si-A20 group; $^{\$\$}P < 0.01$ vs. the si-A20 group)

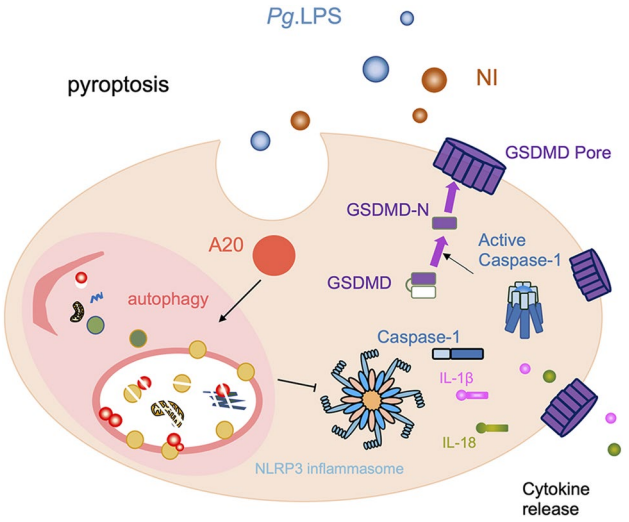

Fig. 7 Schematic diagram depicting A20 modulates NLRP3 inflammasome activation and pyroptosis through autophagy in hPDLCs

expression of Beclin-1 was found in tongue squamous cell carcinoma tissues, especially in tissues with poor prognosis [38]. In our study, multiple evidence indicated that *Pg*.LPS- and NI-induced autophagic flux in hPDLCs, and the overexpression of A20 could amplify the *Pg*.LPS- and NI-induced autophagy.

Autophagy is featured by autophagosome formation and tends to be a pro-survival response to various stresses by processing metabolite and maintain cellular homeostasis [39]. It has been reported that acrolein activated NLRP3 inflammasome mediated-pyroptosis and restricted migration in vascular endothelial cells by ROS-dependent autophagy [28]. Wang X et al. [40] also showed that autophagy modulated acrolein NLRP3-dependent pyroptosis in ZEA-treated INS-1 cells via activation of p65. Previous work confirmed our claim that autophagy could alleviated the increased pyroptosis [41]. We found that *Pg*.LPS and NI activate autophagy and that autophagy could regulate the fate of NLRP3 inflammasome and pyroptosis. Ding et al. [42] have reported that miR-21-5p can relieve pyroptosis and podocyte injury targeting A20 in diabetic nephropathy. Owing to the protective effect of A20, we assumed that A20 may inhibit the activation of NLRP3 inflammasome and pyroptosis. To explore the role of autophagy in the interaction of A20 and pyroptosis in hPDLCs, 3MA and Rapa were utilized. A20 overexpression with LV-A20 reversed the upregulation of pyroptosis and inflammatory cytokines secretion induced by *Pg*.LPS and NI. And when the cells transfected by LV-A20 lentivirus were pre-treated with 3MA or Rapa, pyroptotic cell death and the secretion of cytokines were intensified by 3MA or further reversed by Rapa. The similar treatment on the si-A20 group showed the same trend.

Conclusion

Our results indicated that both the activation of NLRP3 inflammasome and pyroptosis are involved in *Pg*.LPS- and NI-treated hPDLCs. A20 inhibited *Pg*.LPS- and NI-induced pyroptosis and inflammation via enhancing autophagy. In this study, we investigated the roles of pyroptosis and autophagy in the progression of periodontitis, and identified A20 as a potential target for the treatment of periodontitis, which is expected to provide new strategy for the exploration of drugs for the treatment of periodontitis.

Supplementary Information The online version contains supplementary material available at https://doi.org/10.1007/s13577-022-00678-5.

Acknowledgements This work was supported by priority Academic Program Development of Jiangsu Higher Education Institutions, Grant/Award Number: PAPD, 2018-87; National Natural Science Foundation of China, Grant/Award Number: 81771074; Key projects of social development of Jiangsu Department of Science and Technology, Grant/Award Number: BE2020707.

Author contributions HT and YY designed the experiments; YX, YY, and LL were involved in funding acquisition; HT and LH conducted the experiments; SR and YZ were involved in methodology design; HT, LH, and YY analyzed the data; HT and YY prepared the manuscript; YX, LL, YY, and SR reviewed and revised the draft. All authors have read and approved the final manuscript.

Funding This work was supported by priority Academic Program Development of Jiangsu Higher Education Institutions, Grant/Award Number: PAPD, 2018-87; National Natural Science Foundation of China, Grant/Award Number: 81771074; Key projects of social development of Jiangsu Department of Science and Technology, Grant/Award Number: BE2020707.

Availability of data and materials All data generated or analyzed during this study are included in this article.

Declarations

Conflict of interest The authors have no conflicts of interest to declare that are relevant to the content of this article.

Ethical approval The experiments in this article were approved by the Ethical Committee of Nanjing Medical University (NO. 2017-370).

Informed consent All patients and corresponding guardians gave their consents to participate in this study.

References

1. Hajishengallis G, Lamont RJ. Beyond the red complex and into more complexity: the polymicrobial synergy and dysbiosis (PSD) model of periodontal disease etiology. Mol Oral Microbiol. 2012;27:409–19.

2. Naruishi K, Nagata T. Biological effects of interleukin-6 on gingival fibroblasts: cytokine regulation in periodontitis. J cell physiol. 2018;233:6393–400.
3. Genco RJ, Borgnakke WS. Risk factors for periodontal disease (2000). Periodontol. 2013;62:59–94.
4. Johnson GK, Guthmiller JM. The impact of cigarette smoking on periodontal disease and treatment. Periodontol. 2000;2007(44):178–94.
5. Jiang Y, Zhou X, Cheng L, Li M. The impact of smoking on subgingival microflora: from periodontal health to disease. Fron Microbiol. 2000;11:66.
6. Hu Q, Zhang T, Yi L, Zhou X, Mi M. Dihydromyricetin inhibits NLRP3 inflammasome-dependent pyroptosis by activating the Nrf2 signaling pathway in vascular endothelial cells. BioFactors. 2018;44:123–36.
7. Jorgensen I, Miao EA. Pyroptotic cell death defends against intracellular pathogens. Immunol Rev. 2015;265:130–42.
8. Fang Y, Tian S, Pan Y, Li W, Shu Y. Pyroptosis: a new frontier in cancer. Biomed pharmacother. 2019;121:109595.
9. Zeng, Zhaolin, Li, et al. Role of pyroptosis in cardiovascular disease. Cell Prolif. 2019;52:e12563.
10. Wang S, Yuan YH, Chen NH, et al. The mechanisms of NLRP3 inflammasome/pyroptosis activation and their role in Parkinson's disease. Int Immunopharmacol. 2019;67:458–64.
11. Jun HK, Jung YJ, Ji S, An SJ, Choi BK. Caspase-4 activation by a bacterial surface protein is mediated by cathepsin G in human gingival fibroblasts. Cell Death Differ. 2017;25:380–91.
12. Jun HK, Lee SH, Lee HR, Choi BK. Integrin α5β1 activates the NLRP3 inflammasome by direct interaction with a bacterial surface protein. Immunity. 2012;36:755–68.
13. Li C, Yin W, Yu N, Zhang D, Lin L. miR-155 promotes macrophage pyroptosis induced by *Porphyromonas gingivalis* through regulating the NLRP3 inflammasome. Oral Dis. 2019;25:2030–9.
14. Liu W, Liu J, Wang W, Wang Y, Ouyang X. NLRP6 induces pyroptosis by activation of caspase-1 in gingival fibroblasts. J Dent Res. 2018;97:1391–8.
15. Juan Liu YW, Meng H, Jingting Yu, Hongye Lu, Ruifang Lu, Zhao Y, Qi QL, Li S. Butyrate rather than LPS subverts gingival epithelial homeostasis by downregulation of intercellular junctions and triggering pyroptosis. J Clin Periodontol. 2019;46:894–907.
16. Zhuang J, Wang Y, Qu F, et al. Gasdermin-d played a critical role in the cyclic stretch-induced inflammatory reaction in human periodontal ligament cells. Inflammation. 2018;42:548–58.
17. Wang P, Shao BZ, Deng Z, et al. Autophagy in ischemic stroke. Prog Neurobiol. 2018;163–164:98–117.
18. Chengcheng L, Longyi M, Yulong N, et al. The role of reactive oxygen species and autophagy in periodontitis and their potential linkage. Front Physiol. 2017;8:439.
19. Inomata M, Niida S, Shibata KI, Into T. Regulation of Toll-like receptor signaling by NDP52-mediated selective autophagy is normally inactivated by A20. Cel Mol Life Sci. 2012;69:963–79.
20. Chong-Shan S, John HK. TRAF6 and A20 regulate lysine 63-linked ubiquitination of Beclin-1 to control TLR4-induced autophagy. Sci Signal. 2010;3:42.
21. Matsuzawa Y, Oshima S, Takahara M, et al. TNFAIP3 promotes survival of CD4 T cells by restricting MTOR and promoting autophagy. Autophagy. 2015;11(7):1052–62.
22. Catrysse L, Vereecke L, Beyaert R, van Loo G. A20 in inflammation and autoimmunity. Trends Immunol. 2014;35:22–31.
23. Berteau F, Bénédicte R, Aurélien D, et al. Autosomic dominant familial Behet disease and haploinsufficiency A20: a review of the literature. Autoimmun Rev. 2018;17:809–15.
24. Perga S, Martire S, Montarolo F, et al. A20 in multiple sclerosis and Parkinson's disease: clue to a common dysregulation of anti-inflammatory pathways? Neurotox Res. 2017;32:1–7.
25. Navone ND, Perga S, Martire S, et al. Monocytes and CD4+ T cells contribution to the under-expression of NR4A2 and TNFAIP3 genes in patients with multiple sclerosis. J Neuroimmunol. 2014;272:99–102.
26. Walle LV, Opdenbosch NV, Jacques P, et al. Negative regulation of the NLRP3 inflammasome by A20 protects against arthritis. Nature. 2014;512:69–73.
27. Yu P, Wang HY, Tian M, et al. Eukaryotic elongation factor-2 kinase regulates the cross-talk between autophagy and pyroptosis in doxorubicin-treated human melanoma cells in vitro. Acta Pharmacol Sin. 2019;40:1237–44.
28. Chunteng J, Liping, et al. Acrolein induces NLRP3 inflammasome-mediated pyroptosis and suppresses migration via ROS-dependent autophagy in vascular endothelial cells. Toxicology. 2018;410:26–40.
29. O'Brien M, Moehring D, Muñoz-Planillo R, et al. A bioluminescent caspase-1 activity assay rapidly monitors inflammasome activation in cells. J Immunol Methods. 2017;447:1–13.
30. Lork M, Verhelst K, Beyaert R. CYLD, A20 and OTULIN deubiquitinases in NF-κB signaling and cell death: so similar, yet so different. Cell Death Differ. 2017;24:1172–83.
31. Cheng L, Zhang D, Jiang Y, et al. Decreased A20 mRNA and protein expression in peripheral blood mononuclear cells in patients with type 2 diabetes and latent autoimmune diabetes in adults. Diabetes Res Clin Pract. 2014;106:611–6.
32. Cheng YC, Chu LW, Chen JY, et al. Loganin attenuates high glucose-induced schwann cells pyroptosis by inhibiting ROS generation and NLRP3 inflammasome activation. Cells. 2020;9(9):1948.
33. Bai B, Yang Y, Wang Q, et al. NLRP3 inflammasome in endothelial dysfunction. Cell Death Dis. 2020;11(9):776.
34. Miao EA, Rajan JV, Aderem A. Caspase-1-induced pyroptotic cell death. Immunol Rev. 2011;243:206–14.
35. Cheng R, Wu Z, Li M, Shao M, Hu T. Interleukin-1β is a potential therapeutic target for periodontitis: a narrative review. Int J Oral Sci. 2020;12:2.
36. Shi J, Zhao Y, Wang K, et al. Cleavage of GSDMD by inflammatory caspases determines pyroptotic cell death. Nature. 2015;526(7575):660–5.
37. Pei F, Lin H, Liu H, et al. Dual role of autophagy in lipopolysaccharide-induced preodontoblastic cells. J Dent Res. 2015;94:175–82.
38. Wang Y, Wang C, Tang H, et al. Decrease of autophagy activity promotes malignant progression of tongue squamous cell carcinoma. J Oral Pathol Med. 2013;42:557–64.
39. Parzych KR, Klionsky DJ. An overview of autophagy: morphology, mechanism, and regulation. Antioxid Redox Signal. 2014;20:460–73.
40. Wang X, Jiang L, Shi L, Yao K, Liu X. Zearalenone induces NLRP3-dependent pyroptosis via activation of NF-κB modulated by autophagy in INS-1 cells. Toxicology. 2019;428:152304.
41. Meng QH, Li Y, Ji TT, et al. Estrogen prevent atherosclerosis by attenuating endothelial cell pyroptosis via activation of estrogen receptor α-mediated autophagy. J Adv Res. 2020;28:149–64.
42. Ding X, Jing N, Shen A, et al. MiR-21–5p in macrophage-derived extracellular vesicles affects podocyte pyroptosis in diabetic nephropathy by regulating A20. J Endocrinol Invest. 2020;44(6):1175–84.